Ground Non-Linearity Calibration

F. Masci, 4/16/2009, v. 1.0

1. Summary

Below we summarize our analysis of Sample-Up-the-Ramp (SUR) data from the FEB taken during the first MIC2 test for calibrating the non-linearity. Flight Model (FM) test data was acquired on 11-12-2008 and Engineering Model (EM) data on 11-19-2008.

Here's a summary of the delivered products:

```
gndlincal-w1-est-v1.fits
gndlincal-w1-msk-v1.fits
gndlincal-w1-unc-v1.fits

gndlincal-w2-est-v1.fits
gndlincal-w2-msk-v1.fits
gndlincal-w2-unc-v1.fits

gndlincal-w3-est-v1.fits
gndlincal-w3-msk-v1.fits
gndlincal-w3-unc-v1.fits

gndlincal-w4-est-v1.fits
gndlincal-w4-msk-v1.fits
gndlincal-w4-unc-v1.fits
```

where "est" = estimate of non-linearity (quadratic) coefficient; "msk" = calibration mask indicating highly non-linear, very uncertain, and bad ramp-fit pixels; "unc" = 1-sigma uncertainty in non-linearity coefficients.

All the above used the FM electronics data at nominal temperature (as defined at the time - see below). Non-linearity estimates using the EM data are very close to those from FM, albeit slightly smaller (or less non-linear) across all bands: cf. Tables 1 and 2. This could be due to the difference in array temperatures.

This document is organized as follows:

2. Non-linearity Models

<u>Method 1</u>: fitting SUR data at a single fixed illumination close to A/D saturation

An initial analysis of the FEB data for a few pixels revealed that a quadratic correction model was sufficient. This model and the method that uses it was found to be adequate for the *Spitzer* MIPS arrays. The method is based on first fitting the lab SUR data with the following model:

$$y_i = \alpha i^2 + \beta i, \qquad \text{(Eq. 1)}$$

where

$y_i =$ measured SUR value at sample $i = 0, 1, 2 \ldots 8$, and α, β are the fit coefficients.

It is assumed that the SUR data has been zero-baselined so that no intercept is required, i.e., $y_0 = 0$. The ramp intercept at the zeroth sample plays no role in determining the ramp shape.

The parameters α and β are estimated by fitting Eq. 1 to the ramp data y_i for each pixel using χ^2 minimization. The quantity to be minimized is:

$$\chi^2 = \sum_i^N \frac{\left[y_i - \left(\alpha i^2 + \beta i \right) \right]^2}{\sigma_i^2}, \qquad \text{(Eq. 2)}$$

where σ_i are estimates of the uncertainties, e.g., the RMS of repeated exposures from the mean at each ramp sample. Since Eq. 1 is linear in the coefficients, the values of α and β that minimize χ^2 can be written in closed form:

$$\alpha = \frac{K_2 K_5 - K_3 K_4}{K_2^2 - K_1 K_4} \qquad \text{(Eq.3)}$$

$$\beta = \frac{K_2 K_3 - K_1 K_5}{K_2^2 - K_1 K_4},$$

and the error-covariance matrix elements are given by:

$$\sigma_\alpha^2 = \frac{-K_4}{K_2^2 - K_1 K_4} \qquad \text{(Eq.4)}$$

$$\sigma_\beta^2 = \frac{-K_1}{K_2^2 - K_1 K_4}$$

$$\mathrm{cov}(\alpha, \beta) = \frac{K_2}{K_2^2 - K_1 K_4},$$

where:

$$K_1 = \sum_i^N i^4/\sigma_i^2$$

$$K_2 = \sum_i^N i^3/\sigma_i^2$$

$$K_3 = \sum_i^N i^2 y_i/\sigma_i^2$$

$$K_4 = \sum_i^N i^2/\sigma_i^2$$

$$K_5 = \sum_i^N i\ y_i/\sigma_i^2.$$

N is the total number of data points in the fit and can include multiple ramps from repeated exposures at the *same* illumination.

Given that Eq. 1 is fit to specific lab calibration data, we can generalize to any other observed ramp with underlying *linear count rate* β_l by scaling the "time" i at which the linear counts are equal, i.e., if $\beta i = \beta_l i'$ at times i and i', then $i = \beta_l i'/\beta$. We can then transform Eq. 1 into a new generic expression for the counts in a ramp with linear rate β_l.

$$y_{i'} = \left(\frac{\alpha}{\beta^2}\right)\beta_l^2 i'^2 + \beta_l i'. \qquad \text{(Eq. 5)}$$

The assumption of this method should now be apparent: the quantity α/β^2 is assumed to be constant and independent of the incident flux. The parameter α is < 0 since non-linear ramps generally curve downwards. This means the fractional loss in the measured counts at any ramp sample i from the linear expectation is $(\alpha/\beta^2)\beta_l i$. A higher incident flux will therefore suffer a proportionally greater loss at all ramp samples.

The output signal from the DEB is computed on-board from the FEB SUR data y_i as:

$$m = \frac{1}{2^T}\left[O + \sum_{i=0}^{N} c_i y_i\right], \qquad \text{(Eq. 6)}$$

where nominally $N = 8$ samples, O is an offset, c_i are the SUR weighting coefficients, and T is the number of LSBs truncated. A *linear* output signal from the DEB (i.e., assuming a detector was perfectly linear) can be written in terms of the true *linear* ramp count ($\beta_l i$) and SUR coefficients using Eq. 6:

$$m_{lin} = \frac{1}{2^T}\left[\sum_{i=0}^{N} c_i \beta_l i\right], \qquad \text{(Eq. 7)}$$

where it is assumed that a dark along with the DEB bias ($O/2^T$) has been removed. On re-arranging, the true linear rate can be written in terms of the linear DEB signal as follows:

$$\beta_l = \left(\frac{2^T}{\sum_{i=0}^{N} c_i i} \right) m_{lin}. \qquad \text{(Eq. 8)}$$

Substituting Eq. 8 into Eq. 5, we obtain:

$$y_i = \left(\frac{\alpha}{\beta^2} \right) \Omega^2 m_{lin}^2 i^2 + \Omega m_{lin} i, \qquad \text{(Eq. 9)}$$

where

$$\Omega = \frac{2^T}{\sum_{i=0}^{N} c_i i}.$$

Substituting Eq. 9 into the DEB formula (Eq. 6) and rearranging terms, the observed DEB value (m_{obs}) for a pixel can be written in terms of its linearized counterpart (m_{lin}) *after* subtraction of the dark and DEB bias ($O/2^T$) as follows:

$$m_{obs} = C m_{lin}^2 + m_{lin}, \qquad \text{(Eq. 10)}$$

where

$$C = \frac{\alpha}{\beta^2} \frac{2^T \sum_{i=0}^{N} c_i i^2}{\left[\sum_{i=0}^{N} c_i i \right]^2}. \qquad \text{(Eq. 11)}$$

Generally we expect $C \leq 0$ with $C = 0$ implying a perfectly linear response. The quantity C in Eq. 11 is defined as the non-linearity coefficient and is provided (along with its uncertainty and bad-calibration mask) as a FITS image for use in the instrumental calibration (ICAL) pipeline. The 1-sigma uncertainty in C uses the error-covariance matrix in the fit coefficients (Eq. 4). This can be written:

$$\sigma_C = C \left[\frac{\sigma_\alpha^2}{\alpha^2} + \frac{4\sigma_\beta^2}{\beta^2} - \frac{4\,\mathrm{cov}(\alpha,\beta)}{\alpha\beta} \right]^{1/2}. \qquad \text{(Eq. 12)}$$

Eq. 10 can be inverted to solve for the linearized signal m_{lin}:

$$m_{lin} = \frac{2 m_{obs}}{1 + \sqrt{1 + 4 C m_{obs}}} \quad \text{for} \quad m_{obs} \leq -\frac{1}{4C}. \qquad \text{(Eq. 13)}$$

The quantity in the square root is the discriminant:

$$D = 1 + 4 C m_{obs}$$

and we require $D \geq 0$ for a physical solution. This implies there is a maximum observed signal: $m_{obs} = -1/(4C)$ above which a measurement cannot be linearized and hence could not have come from a detector with this non-linearity model. It is very possible that the signal predicted by Eq. 10 turns-over before the maximum of the DEB dynamic range is reached: 32752. Signals satisfying $-1/(4C) < m_{obs} \leq 32752$ therefore cannot be linearized using this model. To avoid (or "soften" the impact of) a possible turn-over, we define the quadratic model solution in Eq. 13 to be only applicable to observed signals $m_{obs} \leq m_{obs}(\max)$, where $m_{obs}(\max)$ is a new calibration parameter. For $m_{obs} > m_{obs}(\max)$, we Taylor expand Eq. 13 about $m_{obs} = m_{obs}(\max)$ to first order and linearly extrapolate to estimate the linearized signal, i.e:

$$m_{lin} \approx m_{lin}(\max) + \left[m_{obs} - m_{obs}(\max)\right] \left.\frac{\partial m_{lin}}{\partial m_{obs}}\right|_{m_{obs} = m_{obs}(\max)}$$

Using Eqs 10 and 13, the linearized signal for observed signals $m_{obs} > m_{obs}(\max)$ can then be written:

$$m_{lin} \approx m_{lin}(\max) + \frac{m_{obs} - m_{obs}(\max)}{2Cm_{lin}(\max) + 1} \quad \text{for} \quad m_{obs} > m_{obs}(\max), \qquad \text{(Eq. 14)}$$

where

$$m_{lin}(\max) = \frac{2m_{obs}(\max)}{1 + \sqrt{1 + 4Cm_{obs}(\max)}}.$$

This extends the flexibility of the quadratic model and is important for characterizing the non-linearity at high observed signals where its effects are most extreme, and there is no guarantee that it follows a pure quadratic. The only caveat is that it introduces a new parameter: $m_{obs}(\max)$. This can be determined graphically provided the calibration data span a large enough dynamic range.

The formalism for estimating uncertainties in linearized signals is described in the ICAL SDS document.

<u>Method 2</u>: fitting SUR data taken at a number of different illuminations spanning full dynamic range

This method is believed to be more direct and trustworthy by the author since it removes the assumption that a single non-linearity coefficient (Eq. 11), as derived from fitting ramp data at a single 'maximal' (unsaturated) illumination, is independent of the illumination level. This new method can therefore provide a check of the above method. For the method to be reliable, we need good illumination sampling over the full observed (DEB) dynamic range.

This method still involves fitting a quadratic model to ramp data using the formalism above, i.e., Eq. 1, except that now it is fit to data at each and every illumination level. This yields a set of "illumination-dependent" coefficients: $(\alpha,\beta)_{I=1}$, $(\alpha,\beta)_{I=2}$, $(\alpha,\beta)_{I=3}$, …

We recall the formula for the observed DEB signal in Eq. 6. After dark subtraction (and consequently removal of the offset $O/2^T$) as performed in the ICAL pipeline, the observed signal can be written in terms of the fit coefficients at any illumination using Eq. 1:

$$m_{obs} = \frac{1}{2^T}\left[\alpha\sum_{i=0}^{N} c_i i^2 + \beta\sum_{i=0}^{N} c_i i\right],$$

or

$$m_{obs} = \frac{\alpha}{2^T}\left[\sum_{i=0}^{N} c_i i^2\right] + m_{lin}, \qquad \text{(Eq. 15)}$$

where

$$m_{lin} = \frac{\beta}{2^T}\sum_{i=0}^{N} c_i i \qquad \text{(Eq. 16)}$$

For every illumination-dependent pair of coefficients $(\alpha,\beta)_I$, we compute corresponding pairs of linearized and (predicted) observed DEB signals $(m_{lin}, m_{obs})_I$ using Eqs 16 and 15 respectively. The (m_{lin}, m_{obs}) pairs are then plotted against each other and a functional relation, $m_{lin} = f(m_{obs})$ between the two is fitted, e.g., a generic polynomial. This fit will also make use of the uncertainties in each of the $(m_{lin}, m_{obs})_I$ as propagated from the uncertainties in $(\alpha,\beta)_I$. For the analysis below, we cannot derive direct functional relations between the $(m_{lin}, m_{obs})_I$ since only 4, 4, 5 and 7 unsaturated illumination levels are available for bands 1,2, 3 and 4 respectively. Furthermore, these only span the low end of the DEB dynamic range.

The beauty of this method is that it explores the non-linearity in DEB space directly, where measurements are made, instead of using functional extrapolations from low to high DEB values from ramp data at a single illumination. It shall be our method of choice in future analyses, provided illuminations over the full dynamic range are available.

3. Analysis Method

All analysis steps were implemented in a self-contained script written in Perl: *lincal_fit*. This script can only be run within the WSDS environment.

1. FEB darks that used the "extended source" were collated for each band and median-combined at each SUR sample. For bands 1 and 2, the median-combined FEB darks looked remarkably flat after the first (unreliable) sample. The band 3 and 4 darks showed a small but significant positive gradient. Therefore, darks were only subtracted from the illuminated data for bands 3 and 4.

2. Before fitting the non-linearity model (e.g., Eq. 1), the ramps were "zero-baselined" to avoid fitting an intercept. This involved medianing all the first sample (intercept) values from all repeated exposures at the same illumination, and subtracting this from all samples in all exposures. In the notation of Section 2, the first sample was

defined at $i = 1$ for bands 1 and 2, i.e., to avoid the unreliable sample at $i = 0$. For bands 3 and 4, the first sample was defined at $i = 0$.

3. As a detail, the band 4 FEB data were first down-sampled by averaging over 2 x 2 pixel blocks in each frame. This will enable the calibration products to be applied to DEB data.

4. FEB data corresponding to the aperture that gave the highest *unsaturated* illumination was initially used for the fitting (see Aperture #'s used in Tables 1 and 2). All repeated FEB exposures at the same illumination were simultaneously fit using a quadratic non-linearity model for every pixel (Eq. 1). The chi-square minimization method described in Section 2 was used. Prior variances (σ_i^2) for each ramp sample y_i were computed from the standard deviation across all repeated exposures at the respective sample for the fixed illumination.

5. The chi-square minimization involved a two-pass process. The first pass estimated the fit parameters α and β and initial estimates of their uncertainties for each pixel. The second pass computed the actual value of the χ^2 metric (Eq. 2). This was used to check for plausibility of the input data uncertainties σ_i. If these happened to be incorrectly estimated on input, then uncertainties in α, β and their covariance will be adversely affected. They therefore need to be adjusted. The χ^2 was redeemed plausible if its value fell within three standard deviations of its expected value: $D_F \pm 3\sqrt{(2D_F)}$, where $\langle\chi^2\rangle = D_F$ = the number of degrees of freedom = number of samples – 2. If outside this range, then it could indicate the presence of outliers in the data, a bad choice of model, or incorrect prior uncertainties (σ_i). Spot checks on large numbers of ramps revealed that the choice of model was adequate overall and that outliers were rare. Therefore, if values of χ^2 were found outside the expected range, the uncertainties in α, β (initially from Eq. 4) were re-adjusted as follows:

$$\sigma_{\alpha \text{ or } \beta} \rightarrow \sigma^{new}_{\alpha \text{ or } \beta} = \sigma_{\alpha \text{ or } \beta} \sqrt{\frac{\chi^2}{D_F}}.$$

This is possible because any factors which are used to inflate or deflate the priors σ_i to ensure plausible χ^2 values can be factored out of the variance formulae for α, β in Eq. 4.

6. Non-linearity calibration coefficients and uncertainties as defined by Eqs. 11 and 12 were then computed. Pixels whose non-linearity estimates were abnormally high, very uncertain, or unreliable as determined from bad ramp fits were tagged in a mask.

4. Results Summary

Tables 1 and 2 compare the non-linearity coefficients as estimated using Eq. 11 from *method 1* for the FM and EM electronics. Only "maximal" source apertures were used in these analyses, i.e., admitting the largest illumination such that all ramps are still below saturation.

	W1	W2	W3	W4
Temp (K)	31.91	31.86	7.76	7.74
Aperture #	6	6	7	10
# Ramps used	20	20	20	10
25th %-tile *C*	-7.41e-06	-1.11e-05	-5.10e-06	-6.12e-06
50th %-tile *C*	-7.15e-06	-1.03e-05	-4.69e-06	-5.79e-06
75th %-tile *C*	-6.90e-06	-9.53e-06	-4.43e-06	-5.63e-06

Table 1: FM electronics non-linearity coefficient (*C* from Eq. 11) percentiles

	W1	W2	W3	W4
Temp (K)	32.13	32.15	7.81	7.75
Aperture #	6	6	7	10
# Ramps used	10	10	10	10
25th %-tile *C*	-7.30e-06	-1.10e-05	-4.84e-06	-5.77e-06
50th %-tile *C*	-7.05e-06	-1.02e-05	-4.57e-06	-5.52e-06
75th %-tile *C*	-6.80e-06	-9.49e-06	-4.36e-06	-5.39e-06

Table 2: EM electronics non-linearity coefficient (*C* from Eq. 11) percentiles

Table 3 compares the percentage non-linearity estimates across all the available apertures (illuminations) using the formalism of *method 2* above. The percentage deviation from non-linearity is defined as:

$$\%NL = 100 * \left(\frac{m_{lin}}{m_{obs}} - 1 \right) \%, \qquad \text{(Eq. 17)}$$

where m_{lin} = linearized median DEB pixel signal and m_{obs} = observed (raw) DEB pixel signal in DN. These $\%NL$ values are also shown in the "D" plots of Section 7. As shown in Table 3, the available FEB ramp data only samples a DEB dynamic range of <~ 12,000 DN for bands 1 and 2, and <~ 18,500 DN for bands 3 and 4.

Aperture # (~illumination)	W1: %NL; m_{obs} (DN)	W2: %NL; m_{obs} (DN)	W3: %NL; m_{obs} (DN)	W4: %NL; m_{obs} (DN)
3	0.81; 1620	1.13; 1509	3.34; 3155	10.29; 10802
4	1.99; 3306	2.76; 3086	4.20; 4362	10.35; 11547
5	4.30; 6509	6.12; 6034	5.27; 6382	10.51; 11151
6	10.84; 12307	15.15; 11158	7.25; 10584	10.70; 11490
7	saturated	saturated	10.62; 18253	10.93; 11892
8	saturated	saturated	saturated	11.64; 13139
10	saturated	saturated	saturated	13.87; 18449

Table 3: Median percentage deviations from linearity (%NL) in median DEB signals (m_{obs}) for different illuminations (or apertures) for FM data alone

5. Masking Criteria

The mask (msk) image products listed in Section 1 indicate those pixels whose non-linearity estimates were abnormally high, very uncertain, unreliable as determined from bad ramp fits, or NaN'd. These conditions are not mutually exclusive. Thresholds were picked by examining outlying populations in pixel histograms of the non-linearity coefficients, S/N ratios of their estimates, and reduced χ^2 values (see plots in Section 7).

Below we summarize thresholds for these quantities and the bad-pixel statistics for each band. Note that only statistics for the active pixel regions are shown. "chi" represents χ^2/dof (i.e., reduced χ^2) where dof = the number of degrees of freedom in the fits (= number of ramp samples from all repeated exposures – 2). The reduced χ^2 values are compared to those expected for a χ^2 distribution with the given dof. Coefficient values > 0 are also declared as bad, i.e., significantly positive values (at many sigma) indicate ramps which are "curving upwards".

FM Electronics

Band 1

Number of "active pix" coeffs < -2.2307141125566e-05 and > 0 = 2015
Number of "active pix" coeffs with S/N < 2 = 670
Number of reduced "active pix" chi-squares with |chi - 1|/sqrt(2/dof) > 50 = 856
Number of "active pix" NaN coeffs = 1

Band 2

Number of "active pix" coeffs < -9.29413461631157e-05 and > 0 = 3168
Number of "active pix" coeffs with S/N < 2 = 520
Number of reduced "active pix" chi-squares with |chi - 1|/sqrt(2/dof) > 100 = 1528
Number of "active pix" NaN coeffs = 5

Band 3

Number of "active pix" coeffs < -2.60834039499969e-05 and > 0 = 1934

Number of "active pix" coeffs with S/N < 2 = 39
Number of reduced "active pix" chi-squares with |chi - 1|/sqrt(2/dof) > 150 = 2130
Number of "active pix" NaN coeffs = 11

Band 4

Number of "active pix" coeffs < -1.51500776070179e-05 and > 0 = 1084
Number of "active pix" coeffs with S/N < 2 = 3
Number of reduced "active pix" chi-squares with |chi - 1|/sqrt(2/dof) > 20 = 1320
Number of "active pix" NaN coeffs = 7

EM Electronics

Band 1

Number of "active pix" coeffs < -2.20363805328816e-05 and > 0 = 1996
Number of "active pix" coeffs with S/N < 2 = 458
Number of reduced "active pix" chi-squares with |chi - 1|/sqrt(2/dof) > 50 = 966
Number of "active pix" NaN coeffs = 1

Band 2

Number of "active pix" coeffs < -9.29669489869412e-05 and > 0 = 3157
Number of "active pix" coeffs with S/N < 2 = 401
Number of reduced "active pix" chi-squares with |chi - 1|/sqrt(2/dof) > 100 = 2159
Number of "active pix" NaN coeffs = 5

Band 3

Number of "active pix" coeffs < -1.92950230484712e-05 and > 0 = 2274
Number of "active pix" coeffs with S/N < 2 = 36
Number of reduced "active pix" chi-squares with |chi - 1|/sqrt(2/dof) > 150 = 2321
Number of "active pix" NaN coeffs = 17

Band 4

Number of "active pix" coeffs < -1.27081617227987e-05 and > 0 = 1123
Number of "active pix" coeffs with S/N < 2 = 6
Number of reduced "active pix" chi-squares with |chi - 1|/sqrt(2/dof) > 50 = 1200
Number of "active pix" NaN coeffs = 8

6. Conclusions and Cautionary Notes

1. The median percentage deviations from linearity across all bands for a *limited range* of DEB signals were summarized in Table 3 for the FM data. Predictions at higher DEB signals using fits to the FEB data are given in the "D" plots of Section 7. At a fiducial DEB signal of 10,000 DN, the non-linearity can be as low as 7% (band 3) and high as 14% (band 2).

2. The bulk of the non-linearity estimates across all pixels in each band are significant to least the 20-σ level ("G" plots in Section 7).

3. The ramp data taken with EM electronics at similar illuminations but with higher array temperatures (by ~0.3-0.5 K) is more linear by ~ 4.5% across all bands. This could be a consequence of the temperature difference. Note that the additional temperature dependent data for the FM set-up (at low and high temperatures) is yet to be analysed.

4. The distribution of the magnitude of non-linearity across pixels is generally very uniform: see Figure 1 and the "E" histograms in Section 7. The largest variations are seen in bands 3 and 4 where the non-linearity systematically increases by ~12% towards the edges. Note that the band 3 and 4 data are contaminated by latents from an earlier test. The residuals are clearly seen in the middle of the band 3 and 4 calibration images in Figure 1.

5. Band-2 is our most "non-linear" band. This also has the greatest number of "badly behaving" ramps and not surprisingly, coincides with the greatest number of bad pixels in general.

6. Bands 3 and 4 show that predictions using fits to data at one illumination, i.e., the highest unsaturated illumination (using method 1) are not consistent with those of method 2 that uses data at all illuminations (see overlayed points in the "D" plots of Section 7). This indicates that the non-linearity coefficient as parameterised by method 1 is illumination dependent, contrary to that found for the *Spitzer* MIPS detectors. However, the two methods agree very well for bands 1 and 2.

7. The non-linearity calibration at high DEB signals is weakly constrained by the FEB lab data. There is a plan to obtain better sampling of the full dynamic range (albeit coarsely in pixel space) on orbit. The non-linearity will be calibrated using the more direct and reliable *method 2*.

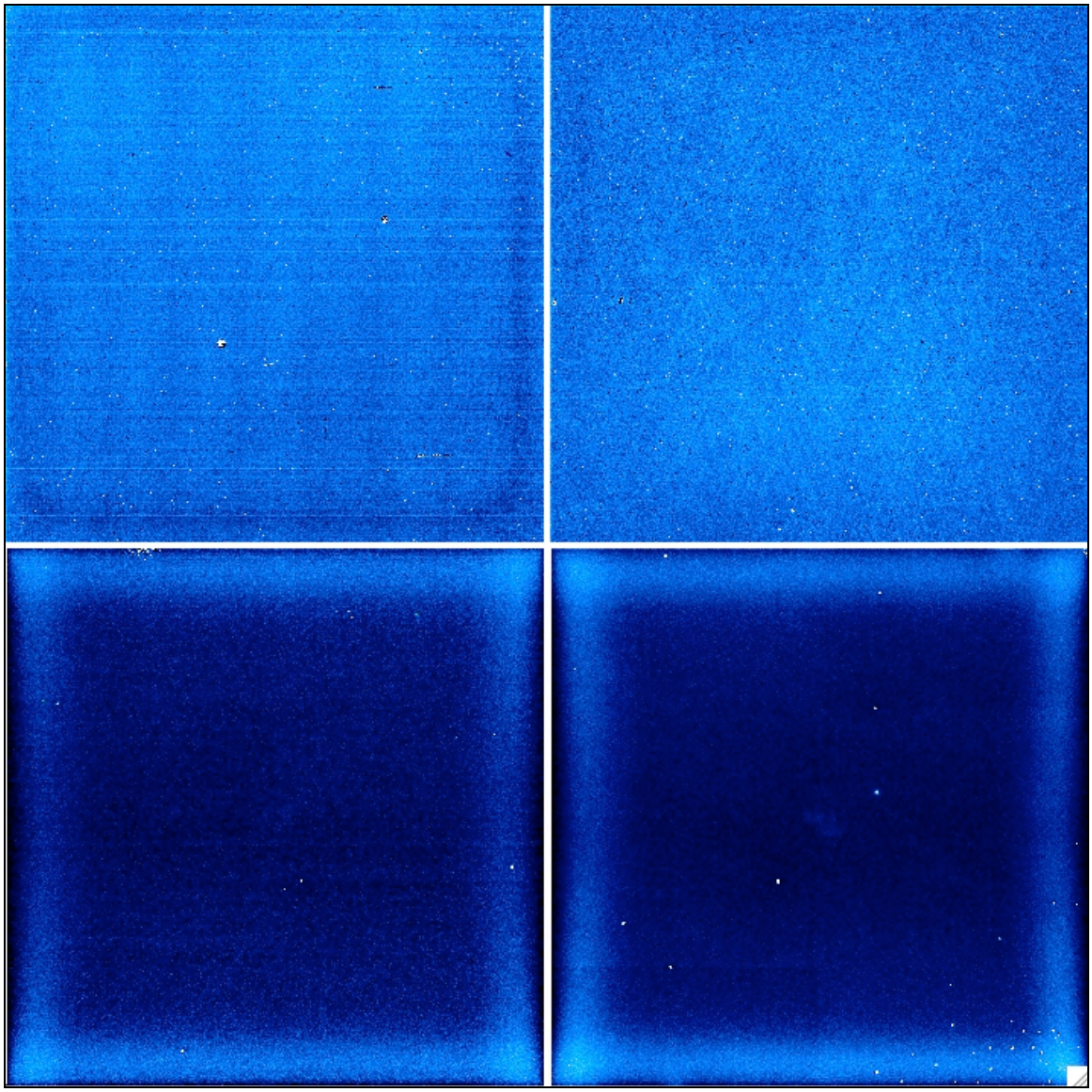

Figure 1: Non-linearity calibration coefficient images (*C* from Eq. 11) for bands 1, 2, 3 and 4: *top left, right; bottom left, right* respectively. Brighter regions correspond to greater non-linearity. All images are at the same stretch.

7. Diagnostic Plots

The plots below pertain to analysis of the FM data. Plots from the EM analysis are available upon request. The plots are labelled **A** through **G** for each band. A description is as follows:

A. FEB ramp values as a function of sample number for a single pixel. Points indicate values from all exposures; blue lines are fits of the quadratic model (Eq. 1), and red lines are the linear component of this fit (βi in Eq. 1). The ramps have been re-baselined to have zero intercept. Band 1 and 2 ramps were forced start at the second FEB sample (due to an unreliable first sample) and hence have 8 samples each. The Band 2 plots also show examples of "bad-pixel" ramps (labelled A2 and A3).

B. 1-sigma dispersion in FEB values versus sample number for a single pixel. These were computed from the standard-deviation in FEB values across all repeated exposures at the fixed illumination. Note the increase in these dispersions with sample number for bands 3 and 4. This is due to the increase in Poisson noise along a ramp at the highest illuminations. The effect is not as great as in bands 1 and 2 since these bands are read-noise dominated. As a consequence, a systematically increasing Poisson noise in a ramp implies that the FEB values there will be weighted down in a χ^2 minimization fit, therefore biasing results. Therefore, inverse variance weighting for the parameter estimation was not used for bands 3 and 4.

C. Predicted linearized DEB signal (in native WISE DN) as a function of observed DEB signal assuming the median non-linearity coefficient for each array (see Table 1). This uses Eqs. 13 and 14 with $m_{obs}(\max) = 18000$ for bands 1 and 2, and $m_{obs}(\max) = 28000$ for bands 3 and 4. There is currently no strong justification for picking these values. They are set according to the available DEB dynamic range in the calibration data and are needed to avoid a pure quadratic model from turning over before the maximum of the dynamic range is reached (see discussion in Section 2).

D. Predicted deviation from linearity (using Eqs. 13, 14, and 17) as a function of observed DEB signal. Blue curves are for the 25th and 75th percentile non-linearity coefficients (top and bottom respectively), and the red curve is for the median non-linearity coefficient (see Table 1). The points are from measurements of the median observed DEB signal at the different illuminations (see Table 3), and use the median coefficient under *method 2* to compute the linearized signal.

E. Histogram of the non-linearity coefficients across all pixels as computed from Eq. 11.

F. Histogram of reduced χ^2 value across pixels with fixed degrees of freedom given by number of samples (typically 180 for FM data) – 2.

G. Histogram of Signal-to-Noise (S/N) ratio in the estimated non-linearity coefficient (Eq. 11 ÷ Eq. 12) across pixels. These values are negative since the non-linearity coefficient for a "normal" non-linear ramp is negative by definition.

Band 1

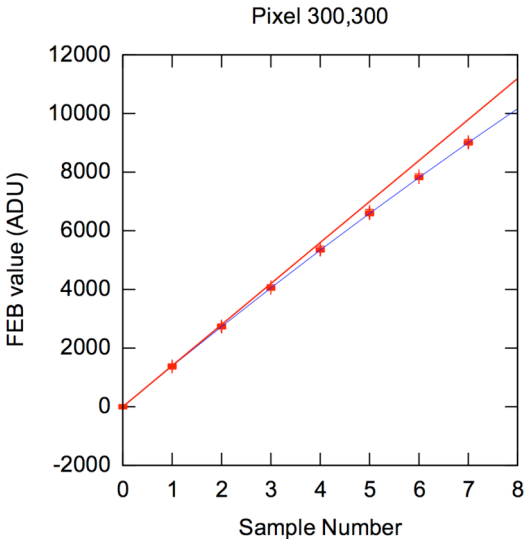
Pixel 300,300
FEB value (ADU)
Sample Number
12000
10000
8000
6000
4000
2000
0
-2000
0 1 2 3 4 5 6 7 8

A

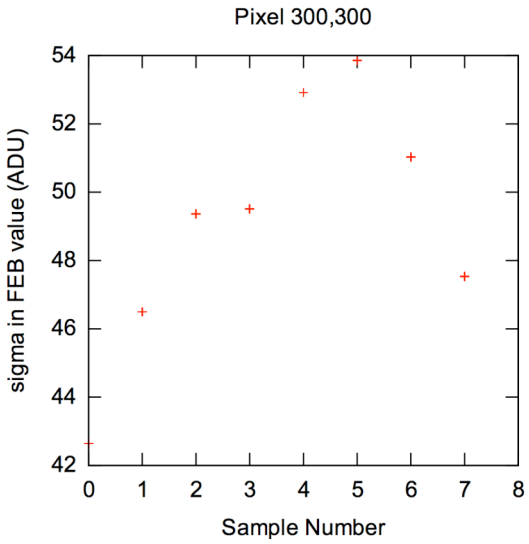
Pixel 300,300
sigma in FEB value (ADU)
Sample Number
54
52
50
48
46
44
42
0 1 2 3 4 5 6 7 8

B

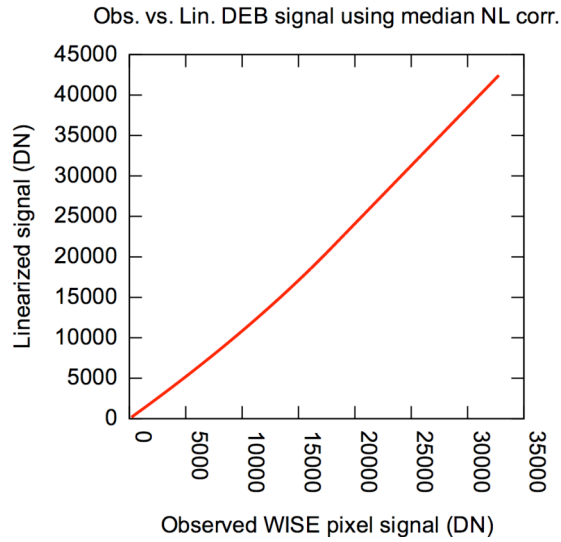
Obs. vs. Lin. DEB signal using median NL corr.
Linearized signal (DN)
Observed WISE pixel signal (DN)
45000
40000
35000
30000
25000
20000
15000
10000
5000
0
0 5000 10000 15000 20000 25000 30000 35000

C

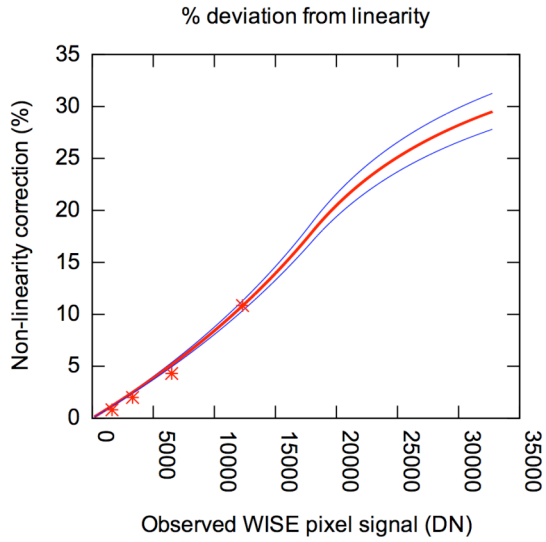
% deviation from linearity
Non-linearity correction (%)
Observed WISE pixel signal (DN)
35
30
25
20
15
10
5
0
0 5000 10000 15000 20000 25000 30000 35000

D

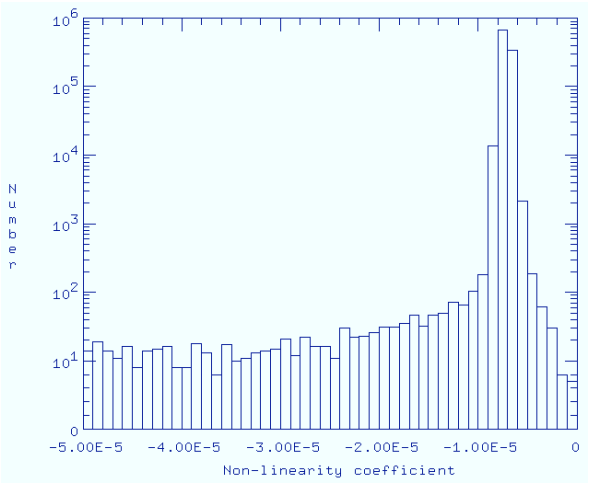

E

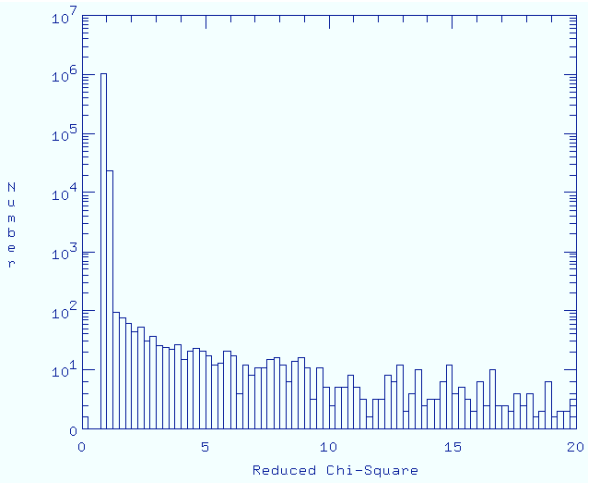

F

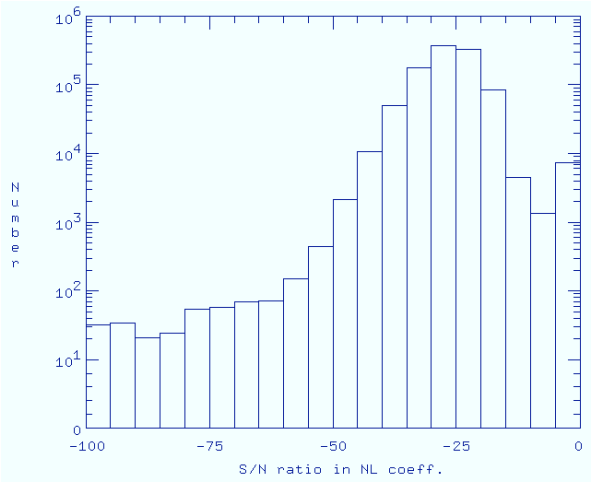

G

Band 2

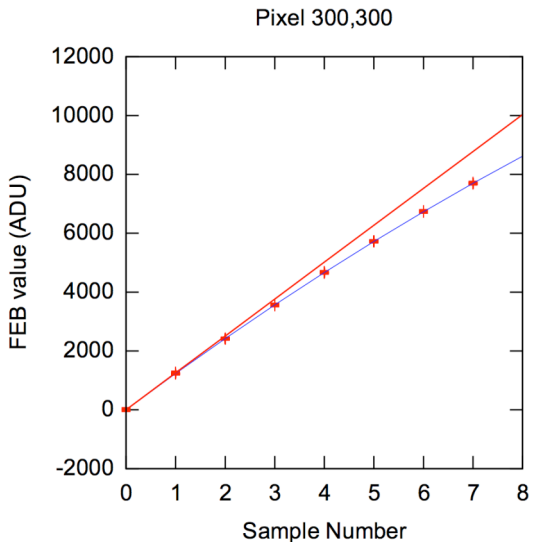

A1

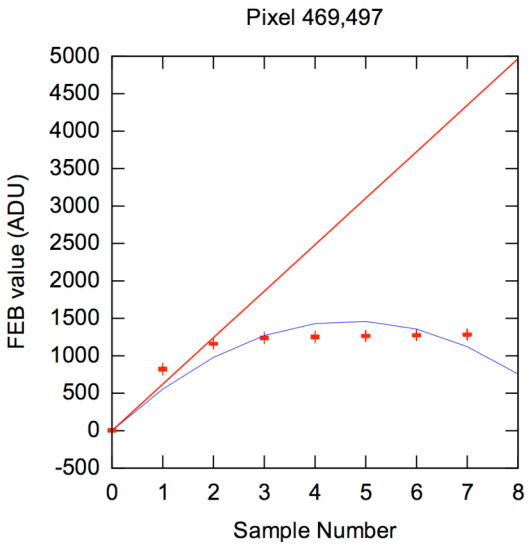

A2

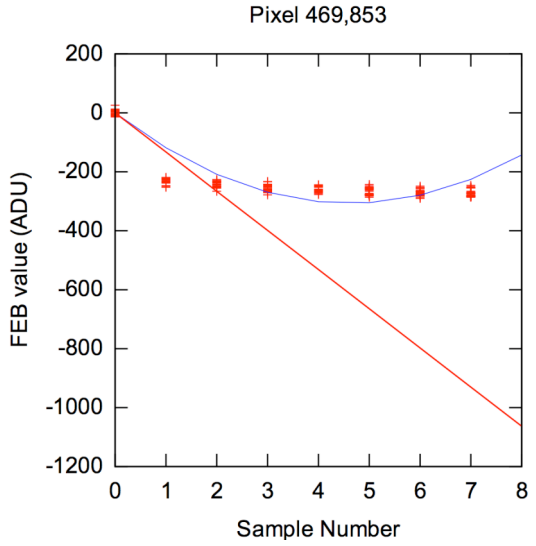
Pixel 469,853
FEB value (ADU)
Sample Number

A3

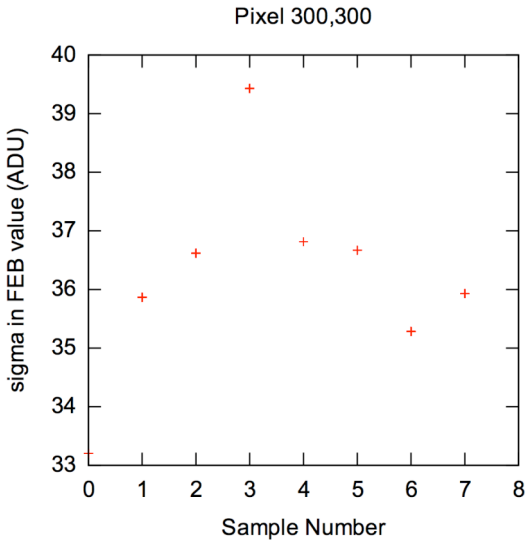
Pixel 300,300
sigma in FEB value (ADU)
Sample Number

B

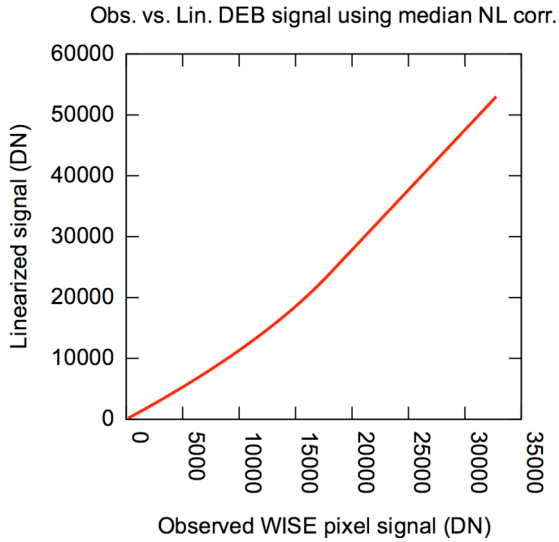
Obs. vs. Lin. DEB signal using median NL corr.
Linearized signal (DN)
Observed WISE pixel signal (DN)

C

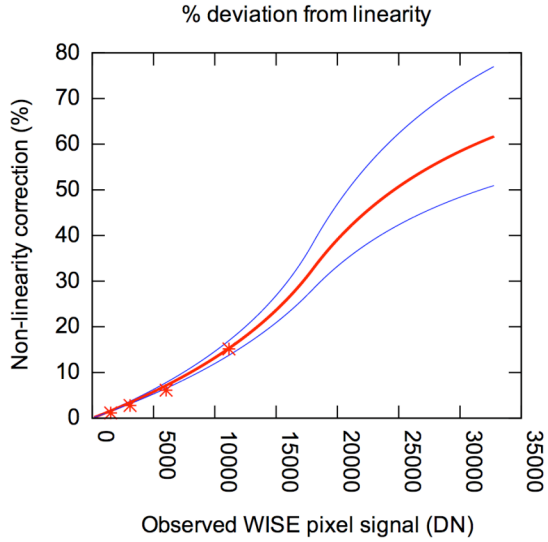
% deviation from linearity
Non-linearity correction (%)
Observed WISE pixel signal (DN)

D

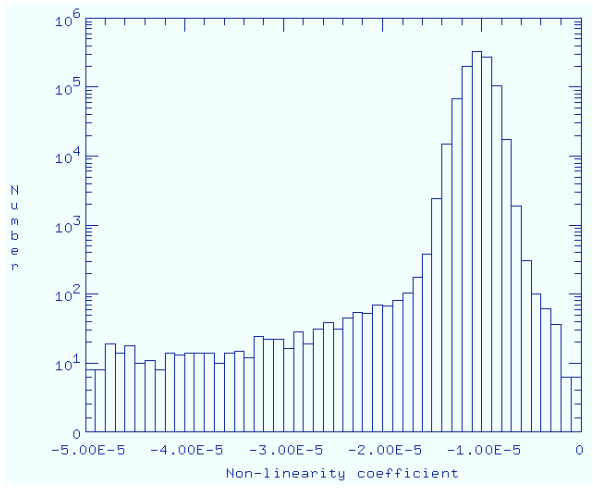
Non-linearity coefficient

E

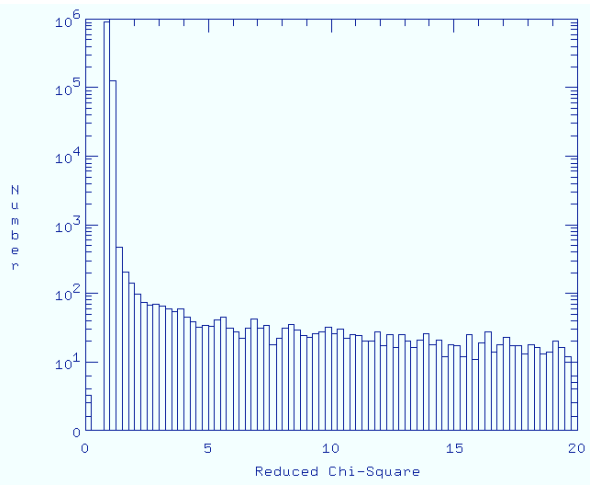
Reduced Chi-Square

F

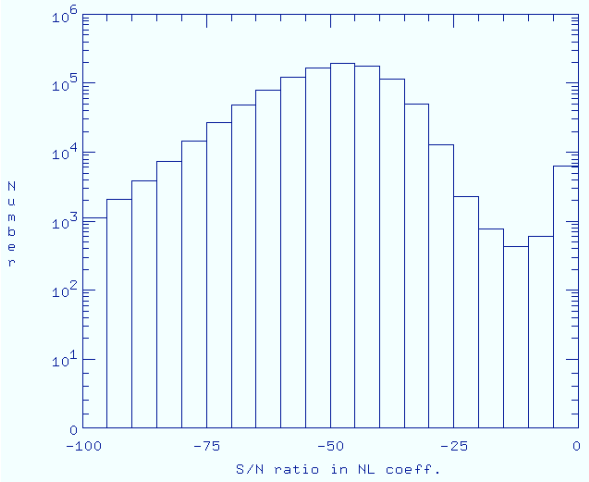
S/N ratio in NL coeff.

G

Band 3

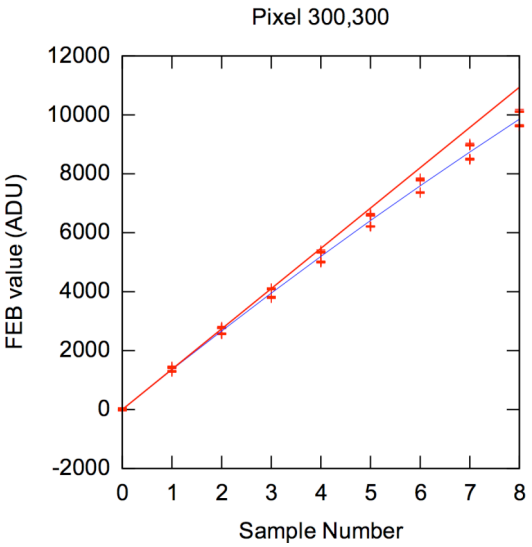
Pixel 300,300
FEB value (ADU)
Sample Number

A

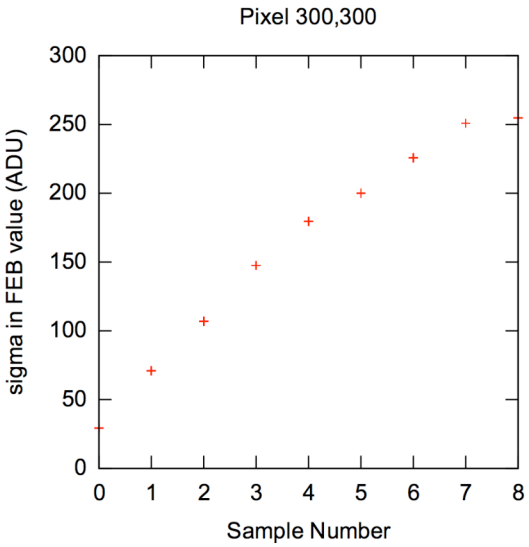
Pixel 300,300
sigma in FEB value (ADU)
Sample Number

B

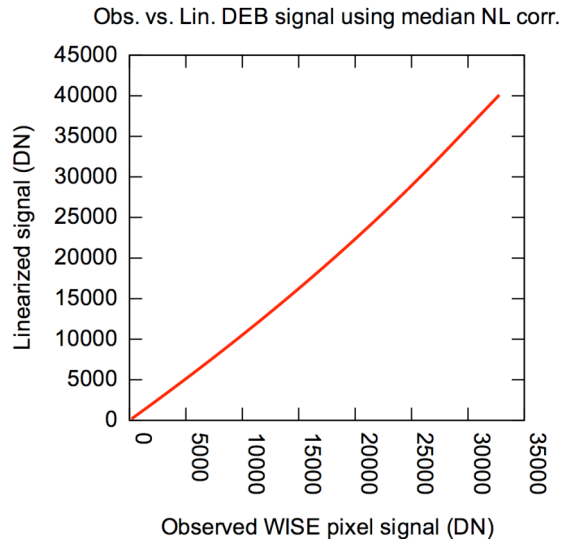
Obs. vs. Lin. DEB signal using median NL corr.
Linearized signal (DN)
Observed WISE pixel signal (DN)

C

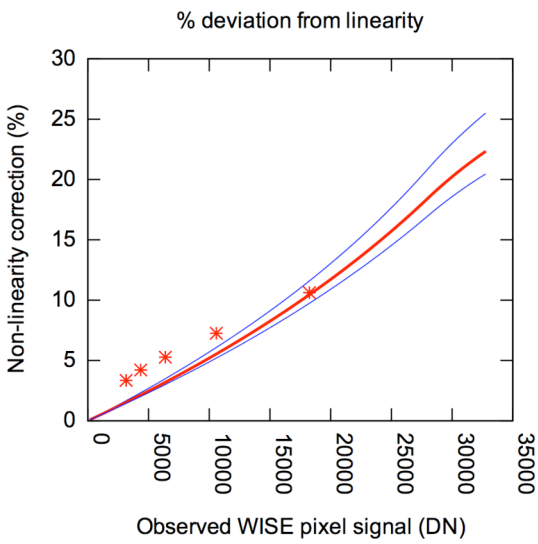
% deviation from linearity
Non-linearity correction (%)
Observed WISE pixel signal (DN)

D

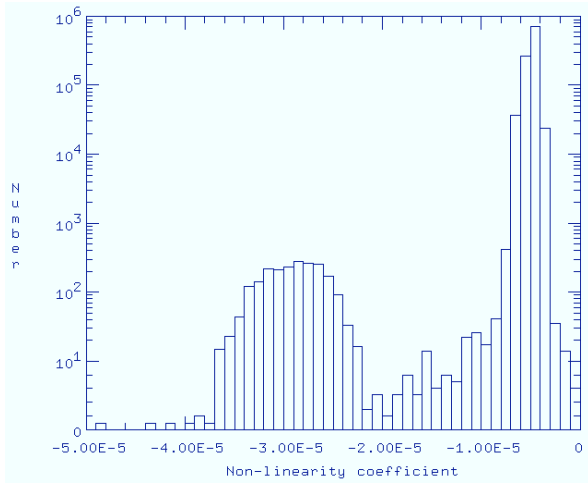
Non-linearity coefficient

E

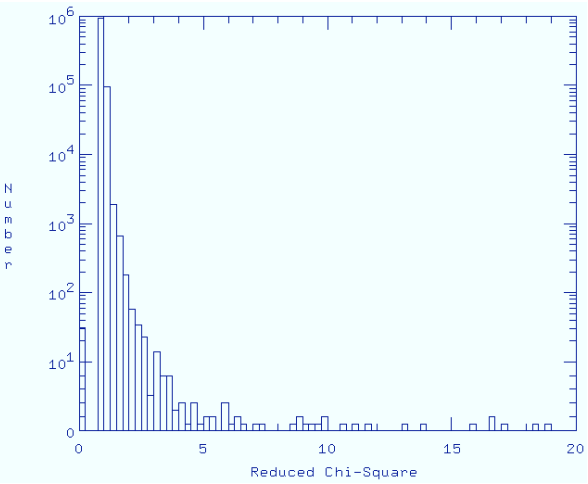
Reduced Chi-Square

F

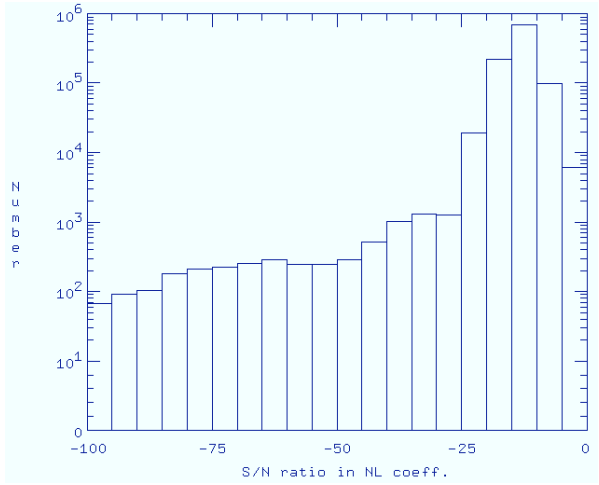
S/N ratio in NL coeff.

G

Band 4

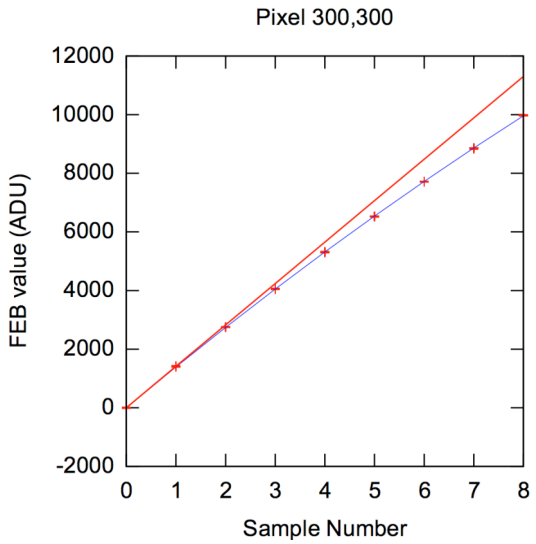
Pixel 300,300
FEB value (ADU)
Sample Number
12000
10000
8000
6000
4000
2000
0
-2000
0 1 2 3 4 5 6 7 8

A

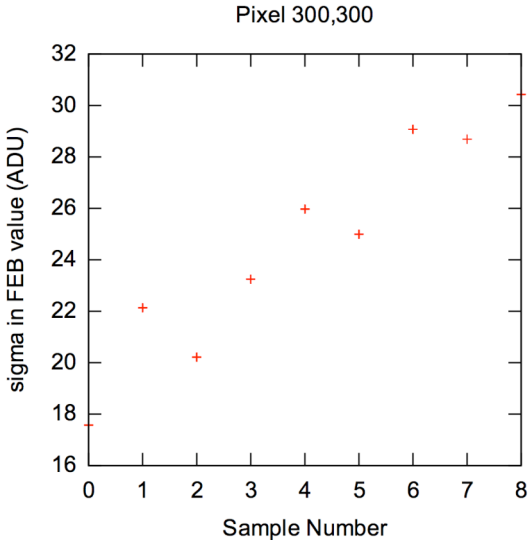
Pixel 300,300
sigma in FEB value (ADU)
Sample Number
32
30
28
26
24
22
20
18
16
0 1 2 3 4 5 6 7 8

B

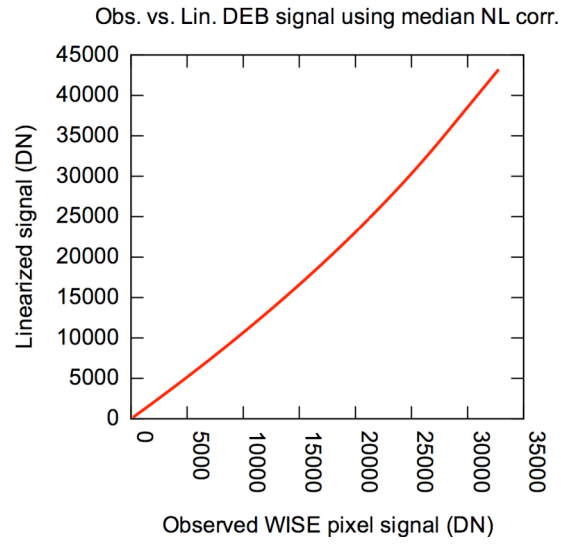
Obs. vs. Lin. DEB signal using median NL corr.
Linearized signal (DN)
Observed WISE pixel signal (DN)
45000
40000
35000
30000
25000
20000
15000
10000
5000
0
0 5000 10000 15000 20000 25000 30000 35000

C

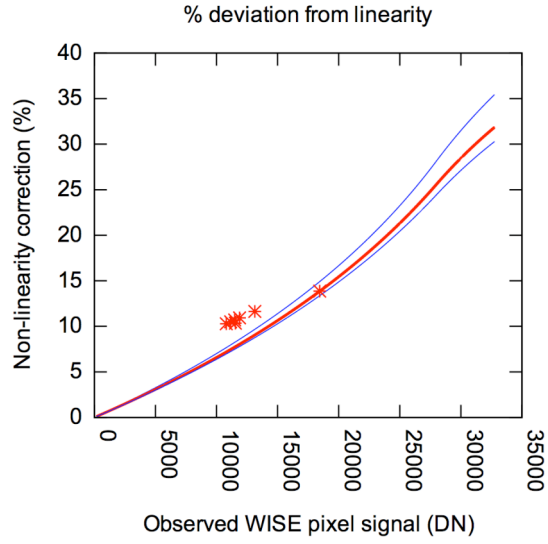
% deviation from linearity
Non-linearity correction (%)
Observed WISE pixel signal (DN)
40
35
30
25
20
15
10
5
0
0 5000 10000 15000 20000 25000 30000 35000

D

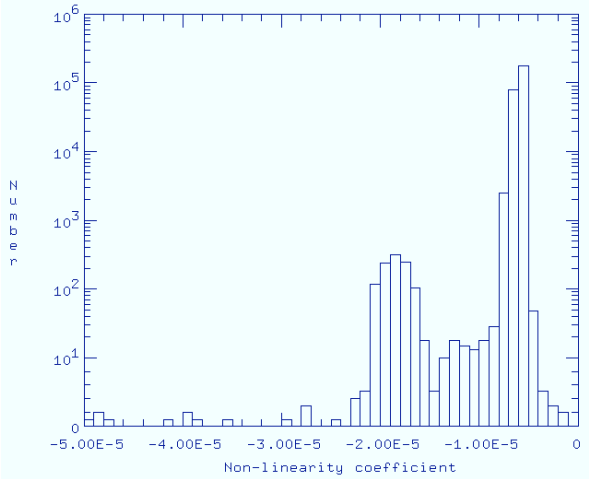
Number
Non-linearity coefficient
-5.00E-5
-4.00E-5
-3.00E-5
-2.00E-5
-1.00E-5
0

E

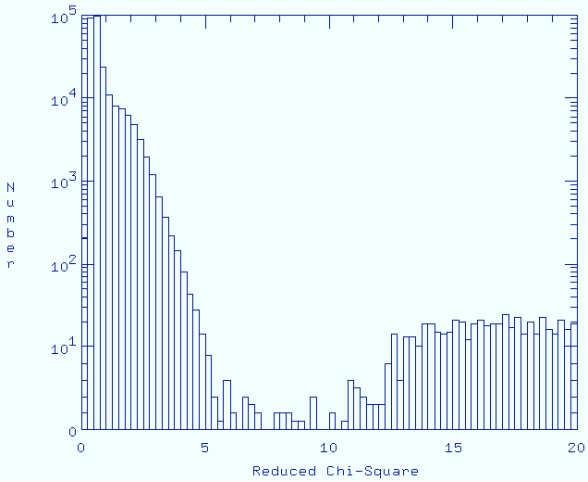
Number
Reduced Chi-Square
0
5
10
15
20

F

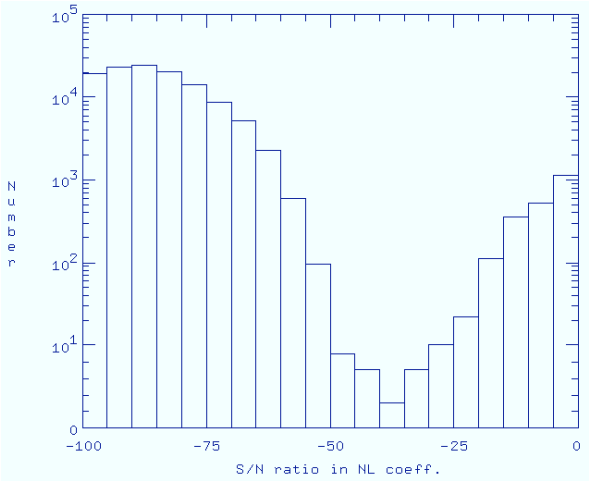
Number
S/N ratio in NL coeff.
-100
-75
-50
-25
0

G